Electronic Journal of Biotechnology 66 (2023) 67–74

Contents lists available at ScienceDirect

Electronic Journal of Biotechnology

journal homepage: www.elsevier.com/locate/ejbt

Research Article

Ginsenoside protects intestinal barrier function and improves epithelium injury in sepsis by regulating the miR-30e-5p/FBXO11 axis

Wenqian Zhu [a,#], Dingjun Fan [b,#], Zhu Zhou [a], Yimei Wang [a], Xiang Huang [a], Liwen Zhang [a], Di Wu [a], Yi Ren [a], Fei Lu [a], Xikun Gao [a,*]

[a] Department of Intensive Care Unit, Changshu Hospital Affiliated to Nanjing University of Chinese Medicine, Changshu City, Jiangsu Province 210023, China
[b] Department of Intensive Care Unit, Changshu Guli People's Hospital, Changshu City, Jiangsu Province 210023, China

GRAPHICAL ABSTRACT

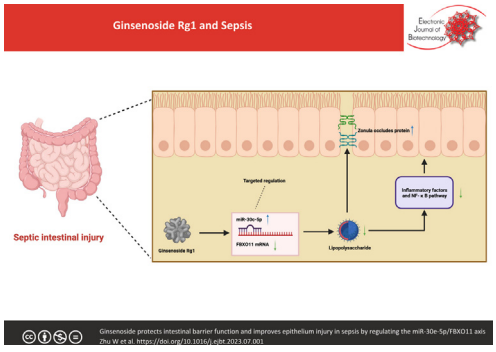

ARTICLE INFO

Article history:
Received 15 February 2023
Accepted 3 July 2023
Available online 20 September 2023

Keywords:
Epithelium injury
FBXO11
Ginsenoside Rg1
Inflammatory cytokines
Inflammatory injury
Intestinal barrier function
Intestinal injury
miR-30e-5p
Sepsis
Tight junction proteins

ABSTRACT

Background: Ginsenoside Rg1 has been studied to improve systemic inflammatory injury induced by sepsis, but its mechanism is not fully understood. The objective of this study was to explore the potential molecular mechanism by which Rg1 ameliorates septic intestinal barrier function impairment.
Results: Rg1 administration or miR-30e-5p upregulation alleviated LPS-induced apoptosis of Caco2 cells, decreased LDH and inflammatory cytokines levels, enhanced cell proliferation, promoted tight junction protein expression, and inhibited p65 phosphorylation. These beneficial effects of Rg1 were compensated by miR-30e-5p knockdown or FBXO11 overexpression. Animal studies have also yielded consistent results. Mechanistically, Rg1 performed this role by upregulating miR-30e-5p and inhibiting FBXO11 expression.
Conclusions: Rg1 protects intestinal barrier function in sepsis by regulating the miR-30e-5p/FBXO11 axis. These data provide new insights into the development of targeted agents for septic intestinal injury and the understanding of Rg1's therapeutic mechanisms.
How to cite: Zhu W, Fan D, Zhou Z, et al. Ginsenoside protects intestinal barrier function and improves epithelium injury in sepsis by regulating the miR-30e-5p/FBXO11 axis. Electron J Biotechnol 2023;66. https://doi.org/10.1016/j.ejbt.2023.07.001.

Peer review under responsibility of Pontificia Universidad Católica de Valparaíso
* Corresponding author.
E-mail address: cssgaoxikun@outlook.com (X. Gao).
# These authors contributed equally to this work.

https://doi.org/10.1016/j.ejbt.2023.07.001
0717-3458/

1. Introduction

Sepsis is a highly complex infectious disease that causes severe systemic inflammation and leads to organ dysfunction [1]. Systemic inflammatory injury and multiple organ dysfunction may further lead to acute gastrointestinal injury [2]. Despite high mortality, fluid/metabolic resuscitation, hemodynamic and end-organ assistance, antibiotic use have made great progress in treating sepsis [3]. Therefore, exploring effective and advanced protective measures for intestinal barrier dysfunction in sepsis has become a research hotspot for scientists.

Ginseng has been used as a dietary supplement and traditional medicine in East Asian countries [4]. As the main component of ginseng, ginsenoside is isolated from red ginseng and white ginseng [5]. Currently, ginsenoside has been found in several studies to improve the systemic inflammatory response mediated by sepsis. For example, ginsenoside Rg1 ameliorates septic acute kidney injury by inhibiting iron sagging in renal tubular epithelial cells [6]. Ginsenoside Rg1 reduces septic apoptosis and inflammation of cardiomyocytes [7]. In addition, ginsenoside Rb1 improves LPS-induced mesenteric venular albumin leakage in rats [8]. However, the underlying mechanism by which ginsenoside Rg1 improves intestinal barrier function remains unclear.

Based on this problem, *in vitro* and *in vivo* models of septic intestinal injury were established to explore the potential mechanism of Rg1 in the treatment of intestinal barrier function impairment. Rg1 is hypothesized to protect the intestinal barrier by regulating the miR-30e-5p/FBOX11 axis. A series of experiments were carried out to verify our conjecture, aiming at discovering novel targets for the treatment of sepsis with Rg1.

2. Materials and methods

2.1. Cell culture

Caco2 cells (ATCC, USA) were prepared in a DMEM mixture (Solarbio, Beijing, China) containing 25 mM HEPES (Solarbio), 15% FBS (Tianhang, Hangzhou, China), 100 U/ml penicillin, 100 mg/ml streptomycin, and 0.25 mg/ml amphotericin B (Sigma, USA) in a humid environment of 37°C and 5% CO_2. To simulate septic intestinal injury, cells were treated with LPS (1 μg/ml, Solarbio) for 24 h. To explore the therapeutic effect of Rg1, cells were treated with 10 μM Rg1 after 30 min LPS treatment.

2.2. Cell transfection

MiR-30e-5p mimic/inhibitor, si-FBXO11, pcDNA 3.1-FBXO11, and negative controls (RiboBio, China) were transfected into Caco2 cells using Lipofectamine 2000 (Invitrogen). RT-qPCR or Western blot was utilized to evaluate the transfection efficiency after 48 h.

2.3. LDH detection

Caco2 cells were inoculated into 96-well plates, and the culture supernatant was collected. LDH release was then tested using the LDH release detection kit (Beyotime, Shanghai, China). OD value at 495 nm was detected by enzyme marker.

2.4. CCK-8

Caco2 cells were inoculated on 96-well plates overnight and treated at 37°C for 2 h using CCK-8 solution (Dojindo, Kuamoto, Japan). Absorbance was measured at 450 using a multifunctional microplate reader, SpectraMax M5 (Molecular Devices, USA).

2.5. Flow cytometry

Caco2 cells were collected using EDTA-free trypsin, centrifuged at 1600 × *g* for 5 min, rinsed twice with PBS, followed by staining with 5 μL Fluorescein isothiocyanate Annexin V and 5 μL propidium iodide (KGA106, Keygen, Nanjing, China) for 15 min. Apoptosis was then examined by flow cytometry (BD Biosciences, USA).

2.6. Dual luciferase reporting experiment

To verify miR-30e-5p binding to the FBXO11 3′UTR region, dual luciferase reporter assay was performed. FBXO11 3′UTR was amplified by PCR using genomic DNA from Caco2 cells and cloned into the psiCHECK2 vector (Promega, USA), named WT-FBXO11. The mutation was inserted into the miR-30e-5p binding region in the FBXO11 3′UTR and named MUT-FBXO11. Lipofectamine 2000 (Invitrogen) was utilized to co-transfect the above reporter vector and miR-30e-5p mimic or mimic NC into Caco2 cells. Luciferase activity was measured using the dual luciferase Reporter Assay System (Promega).

2.7. RIP experiment

RIP was detected using Magna RIP kit (Millipore). In simple terms, Caco2 cells were digested using RIP buffers, and extracts were cultured using magnetic beads that bind to anti-IgG or anti-Ago2. Then, the immunoprecipitated RNA was purified and its enrichment was analyzed by RT-qPCR.

2.8. CLP animal model

Animal study has been approved by the Animal Ethics Committee of Changshu Hospital Affiliated to Nanjing University of Chinese Medicine. A total of 100 male C57BL/6J mice (8–12 weeks of age) were purchased from Hunan SJA Laboratory Animal Co., Ltd. Mice were raised in specific pathogen-free laboratories (60–65% humidity, 22–24°C, food and water supply, 12 h light/dark cycle). After one week of adaptive feeding, mice were treated with CLP to establish a sepsis model [9]. In short, the mice were anesthetized and placed in a supine position. The cecum was then slightly pulled out through a midline incision in the abdominal wall, the fecal matter from the upper cecum was squeezed, and the blood vessels on the mesenteric surface were separated. Next, sterile No. 4 thread was used to ligate the midpoint between the cecal valve and the cecum, and a 21G sterile needle was used to pierce the wall of the cecum at the midpoint between the ligation site and the top of the cecum, resulting in a perforation. The cecum slightly was squeezed to make sure the perforation is clear. After laparotomy, the cecum of the sham mice was gently pulled out without ligature and re-located in the abdominal cavity, which was then closed and sutured layer by layer. Liquid resuscitation was performed with 1 ml PBS before abdominal closure. Rg1 (20 mg/kg) was injected intravenously 30 min after surgery [10]. All CLP mice developed severe sepsis symptoms within 24 h, and most died within 48 h. To silence miR-30e-5p, mmu-miR-30e-5p antagomir (80 mg/kg for three days) was injected into mice through a caudal vein one week before CLP surgery. Twenty-four hours after CLP operation, 10 mice in each group were euthanized, and blood and colon tissues were collected. Tissues were fixed with 4% paraformaldehyde or preserved at −80°C. The remaining mice in each group were tested for animal survival 48 h later.

2.9. Biochemical index detection

LPS, TNF-α, IL-1β, and IL-6 were tested using commercial kits (Nanjing Jiancheng Bioengineering Institute & Thermo Fisher Scientific).

2.10. HE staining

Mouse colon tissues were embedded in paraffin and dewaxed by gradient dehydration. After soaking in Harris Hematoxylin for 3–8 min, the tissues were washed under running water, differentiated for a few seconds with 1% hydrochloric acid alcohol, washed under running water, and treated with 0.6% ammonia. Next, the tissues were stained with eosin for 1–3 min, air-dried, and sealed with a neutral glue. Images were taken during microscopy to analyze intestinal pathology.

2.11. TUNEL staining

Apoptotic cells in colon tissues were analyzed using One-Step TUNEL Apoptosis Assay kit (Roche). Paraffin sections of the colon were dewaxed, hydrated, treated with protease K for 20 min, and incubated for 1 h with a mixture of fluorescence-labeled dUTP solution and TdT enzymes in a humidified environment at 37°C. DNase I treatment and dUTP treatment were considered positive control and negative control, respectively. Subsequently, the colon tissue was treated with diaminobenzidine with DAPI (Sigma-Aldrich; Merck KGaA), followed by gradient ethanol, xylene, and neutral balsam. The images were observed using a microscope (Carl Zeiss, LSM700).

2.12. RT-qPCR

Total RNA was extracted from tissues or cells using a TRIzol kit (16096020 or AM1561, Thermo Fisher). Subsequently, 5 μg RNA was reverse-transcribed according to the RT-qPCR kit (RR047A, Takara, Japan), which was then performed in the ABI PRISM 7300 RT-PCR system (Applied Biosystems, USA) using a rapid SYBR Green PCR kit for qPCR. U6 and GAPDH were endogenous control genes of miRNA and mRNA, respectively. $2^{-\Delta\Delta Ct}$ was utilized to calculate relative gene expression. The primer sequence is shown in Table 1.

2.13. Western blot

Tissues and cells were lysed by enhanced radioimmunoprecipitation lysis buffer (Boster, Wuhan, China) containing a protease inhibitor, and the product was quantified for protein concentration using the BCA Assay kit (Boster). Protein was then isolated using 10% SDS-PAGE, transferred to a polyvinylidene fluoride membrane, which was sealed with 5% bovine serum albumin for 1 h and incubated overnight with diluted primary antibody at 4°C. Next, the membrane was combined with a horseradish peroxidase-labeled secondary antibody (goat anti-rabbit, ab205718, 1:10000; Goat anti-mouse, 1:10000; ab205719) at room temperature for 1 h, and protein bands were detected using an ECL chemiluminescence kit (EMD Millipore). Gray values were evaluated by Image J gel image analysis software. Primary antibodies: ZO-1 (21773-1-AP, Proteintech), occludin (13409-1-AP, Proteintech), cleaved caspase-3 (ab32042, Abcam), p-p65 (3039, CST), GAPDH (60004-1-Ig, Proteintech).

Table 1
PCR primer sequences.

	primer sequences (5′ - 3′)
FBXO11	Forward: 5′- CACCACAATGCACACCACTG-3′ Reverse: 5′- ATGGTGGGACATGCTCCTTG-3′
miR-30e-5p	Forward: 5′- GCGCTGTAAACATCCTTGAC -3′ Reverse: 5′- TGGTGTCGTGGAGTCG-3′
U6	Forward: 5′- CTCGCTTCGGCAGCACA-3′ Reverse: 5′- AACGCTTCACGAATTTGCGT-3′
GAPDH	Forward: 5′- CACCCACTCCTCCACCTTTG-3′ Reverse: 5′- CCACCACCCTGTTGCTGTAG-3′

2.14. Data analysis

All experiments were performed independently at least 3 times. Statistical analysis was performed using GraphPad Prism 9.0 software. Data were expressed as mean ± standard deviation (SD). Student t test compared the difference between two groups, one-way analysis of variance compared that difference among multiple groups, and Tukey HSD compared pairwise difference. $P < 0.05$ was statistically significant.

3. Results

3.1. Rg1 improves intestinal barrier dysfunction and epithelium injury induced by LPS

LPS-injured Caco2 cells were treated with Rg1. LDH levels were first assessed using a commercial kit. LPS treatment promoted LDH release, while Rg1 reduced LDH release (Fig. 1A). CCK-8 method showed that LPS treatment reduced cell viability, but Rg1 restored cell viability (Fig. 1B). Flow cytometry determined that LPS promoted apoptosis, but Rg1 reduced it (Fig. 1C). In addition, LPS increased levels of TNF-α, IL-1β, and IL-6 in cells, while Rg1 reduced levels of these inflammatory cytokines (Fig. 1D). Western blot observed that LPS inhibited ZO-1 and occludin protein expression and increased cleaved caspase-3 and p-p65 protein expression, while Rg1 administration effectively alleviated changes in these proteins (Fig. 1E).

3.2. miR-30e-5p improves intestinal barrier dysfunction and epithelium injury

miR-30e-5p mimic was transfected into LPS-treated Caco2 cells. LPS inhibited miR-30e-5p, but miR-30e-5p mimic restored miR-30e-5p expression (Fig. 2A). Gain-of-function experiments demonstrated that restoring miR-30e-5p could reduce LDH release (Fig. 2B), increase cell viability (Fig. 2C), and reduce cell apoptosis rate (Fig. 2D). In addition, overexpressing miR-30e-5p decreased levels of TNF-α, IL-1β, and IL-6 (Fig. 2E), promoted ZO-1 and occludin protein expression, and inhibited cleaved caspase-3 and p-p65 expression levels (Fig. 2F).

3.3. Rg1 improves LPS-mediated intestinal barrier function impairment by promoting miR-30e-5p expression

miR-30e-5p inhibitor was transfected at the same time of Rg1 administration. Rg1 administration enhanced miR-30e-5p expression (Fig. 3A). Functional rescue tests checked that Rg1 administration decreased LDH release, encouraged cell proliferation, decreased apoptosis and levels of inflammatory cytokines, elevated ZO-1 and occludin, and inhibited cleaved caspase-3 and p-p65 expression. However, these therapeutic effects of Rg1 were weakened by miR-30e-5p inhibitor (Fig. 3B-F).

3.4. MiR-30e-5p targets FBXO11

Bioinformatics website starbase predicted potential binding sites for miR-30e-5p and FBXO11 (Fig. 4A). Subsequently, the tar-

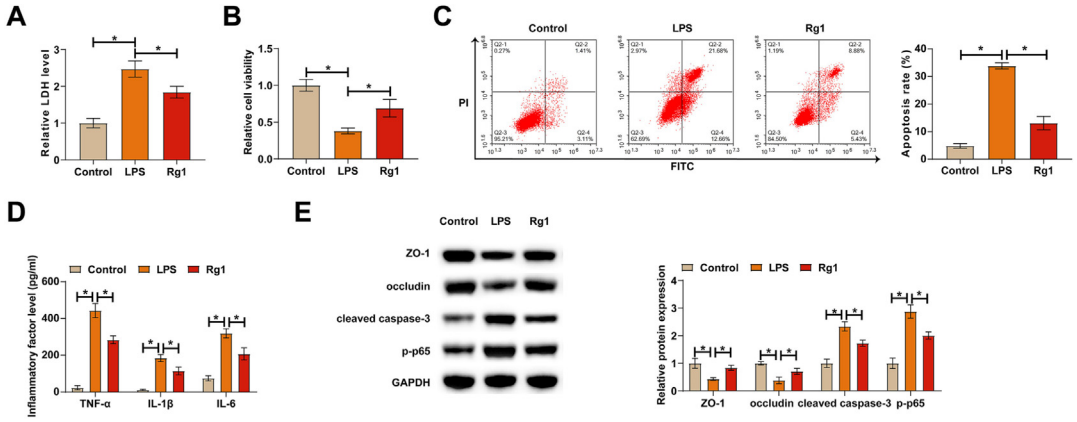

Fig. 1. Rg1 improves intestinal barrier dysfunction and cell damage induced by LPS. Rg1 was treated in LPS-induced Caco2 cells. (A) LDH release detected by commercial kit; (B) Cell viability detected by CCK-8 method; (C) Apoptosis analyzed by flow cytometry; (D) Inflammatory cytokines measured by ELISA kits; (E) ZO-1, occludin, cleaved caspase-3, and p-p65 detected by Western blot. Data were expressed as mean ± SD (N = 3). * $P < 0.05$.

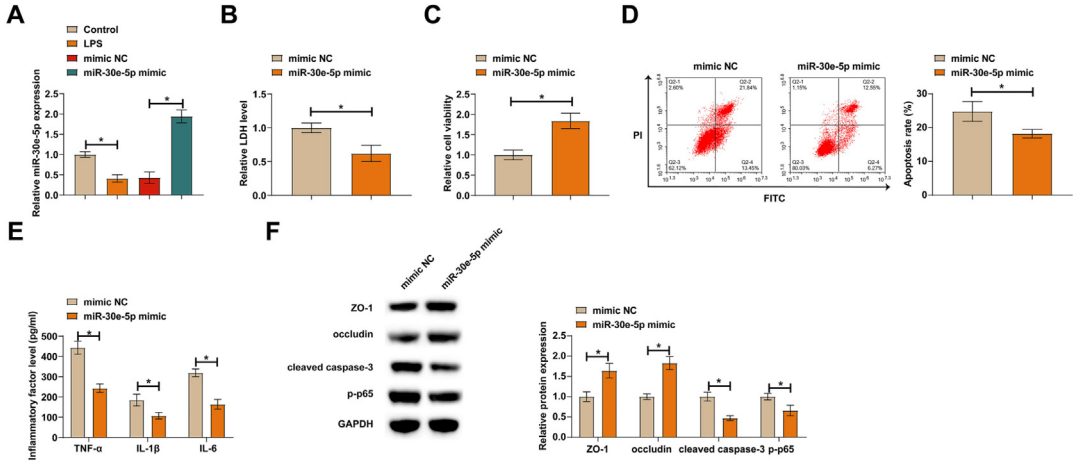

Fig. 2. miR-30e-5p improves intestinal barrier dysfunction and cell damage. miR-30e-5p mimic was transfected into LPS-injured Caco2 cells. (A) miR-30e-5p expression detected by RT-qPCR; (B) LDH release detected by commercial kit; (C) Cell viability detected by CCK-8 method; (D) Apoptosis analyzed by flow cytometry; (E) Inflammatory cytokines measured by ELISA kits; (F) ZO-1, occludin, cleaved caspase-3, and p-p65 detected by Western blot. Data were expressed as mean ± SD (N = 3). * $P < 0.05$.

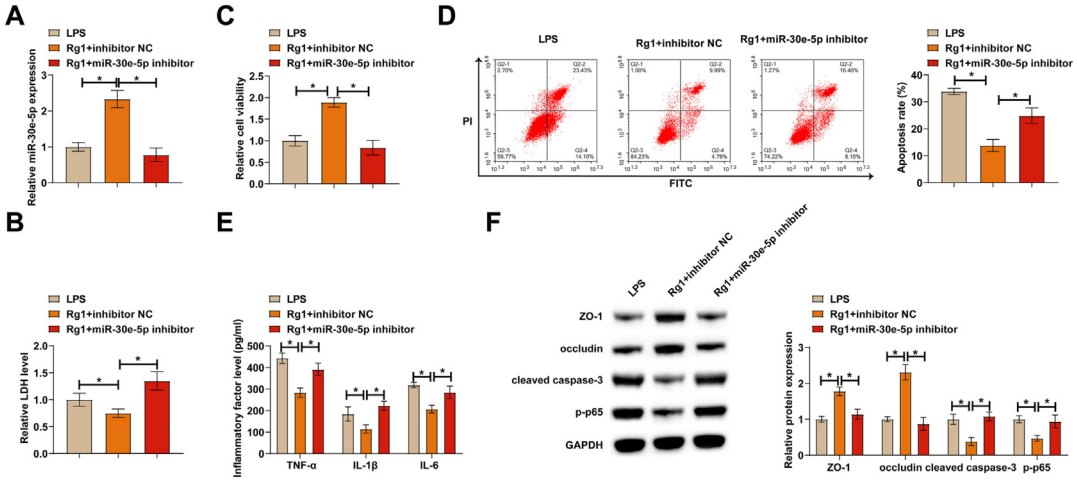

Fig. 3. Rg1 improves LPS-mediated intestinal barrier function impairment by promoting miR-30e-5p expression. In LPS-treated Caco2 cells, Rg1 was administered while transfecting with miR-30e-5p inhibitor. (A) miR-30e-5p expression detected by RT-qPCR; (B) LDH release detected by commercial kit; (C) Cell viability detected by CCK-8 method; (D) Apoptosis analyzed by flow cytometry; (E) Inflammatory cytokines measured by ELISA kits; (F) ZO-1, occludin, cleaved caspase-3, and p-p65 detected by Western blot. Data were expressed as mean ± SD (N = 3). * $P < 0.05$.

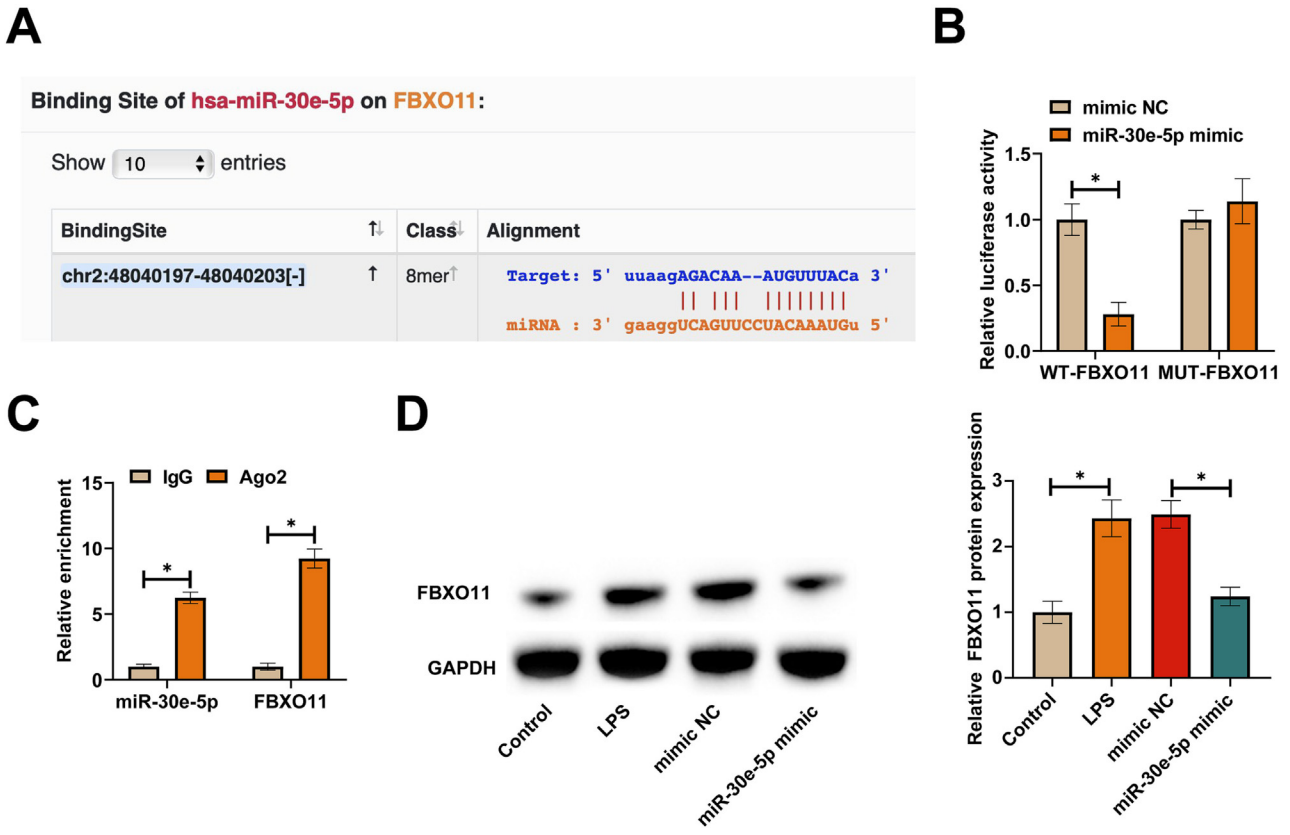

Fig. 4. Targeted regulation of FBXO11 by MiR-30e-5p. (A) Bioinformatics website starbase predicted the potential binding sites of miR-30e-5p and FBXO11; (B) Dual luciferase reporting assay verified the targeting relationship between miR-30e-5p and FBXO11; (C) RIP experiment verified the binding relationship between miR-30e-5p and FBXO11; (D) FBXO11 expression detected by western blot. Data were expressed as mean ± SD (N = 3). * $P < 0.05$.

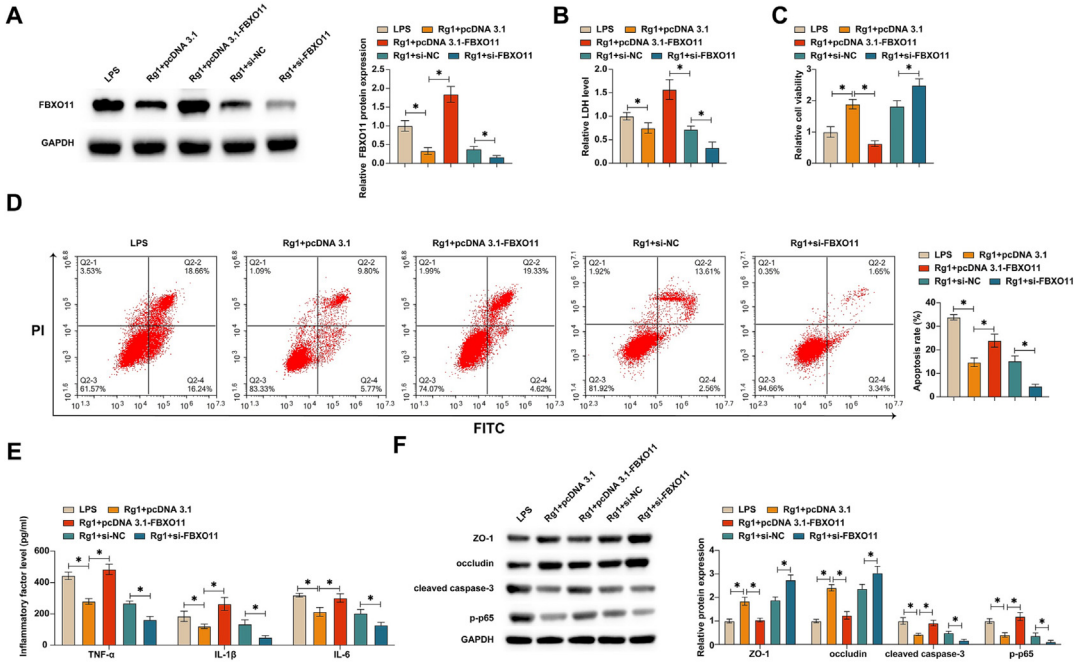

Fig. 5. Rg1 improves LPS-mediated impairment of intestinal barrier function by regulating miR-30e-5p/FBXO11 axis. In LPS-treated Caco2 cells, pcDNA 3.1-FBXO11 or si-FBXO11 was transfected while Rg1 was administered. (A) FBXO11 expression detected by Western blot; (B) LDH release detected by commercial kit; C: Cell viability detected by CCK-8 method; (D) Apoptosis analyzed by flow cytometry; (E) Inflammatory cytokines measured by ELISA kits; (F) ZO-1, occludin, cleaved caspase-3, and p-p65 detected by Western blot. Data were expressed as mean ± SD (N = 3). * $P < 0.05$.

geting relationship between miR-30e-5p and FBXO11 was analyzed by dual luciferase reporting assay and RIP assay. As presented in Figs. 4B-4C, co-transfection of WT-FBXO11 and miR-30e-5p mimic could reduce luciferase activity, and FBXO11 and miR-30e-5p were highly enriched in Ago2 magnetic beads. Next, FBXO11 expression was examined in intestinal injury. Western blot results highlighted that LPS raised FBXO11 expression, but overexpressing miR-30e-5p blocked FBXO11 levels (Fig. 4D).

3.5. Rg1 improves LPS-mediated impairment of intestinal barrier function by regulating the miR-30e-5p/FBXO11 axis

pcDNA 3.1-FBXO11 or si-FBXO11 was transfected while Rg1 was administered. Rg1 administration suppressed FBXO11 protein levels, but pcDNA 3.1-FBXO11 restored FBXO11 protein levels, and si-FBXO11 further reduced FBXO11 protein expression (Fig. 5A). According to the above results, Rg1 administration had therapeutic effects on LPS-injured Caco2 cells. However, FBXO11 overexpression attenuated these therapeutic effects of Rg1, and knockdown of FBXO11 enhanced the protective effect of Rg1 against LPS-induced intestinal epithelial cell injury (Fig. 5B-F).

3.6. Rg1 improves ClP-mediated impairment of intestinal barrier function by regulating the miR-30e-5p/FBXO11 axis

Subsequently, animal experiments were conducted to verify the results of cell experiments. RT-qPCR and Western blot recognized that CLP increased FBXO11 and inhibited miR-30e-5p levels, while Rg1 administration reversed this phenomenon. miR-30e-5p antagomir increased FOXB11 and inhibited miR-30e-5p levels (Fig. 6A-B). Survival analysis showed that CLP surgery resulted in increased mortality in mice, and Rg1 administration reduced mortality in mice, but miR-30e-5p knockdown impaired the therapeutic effect of Rg1 (Fig. 6C). Biochemical analysis showed that Rg1 administration reduced serum LPS levels and intestinal inflammatory cytokines, which were weakened by knockdown of miR-30e-5p (Fig. 6D). HE and TUNEL staining viewed that Rg1 administration reduced intestinal inflammatory damage and apoptosis of intestinal epithelial cells, while miR-30e-5p downregulation reduced the therapeu-

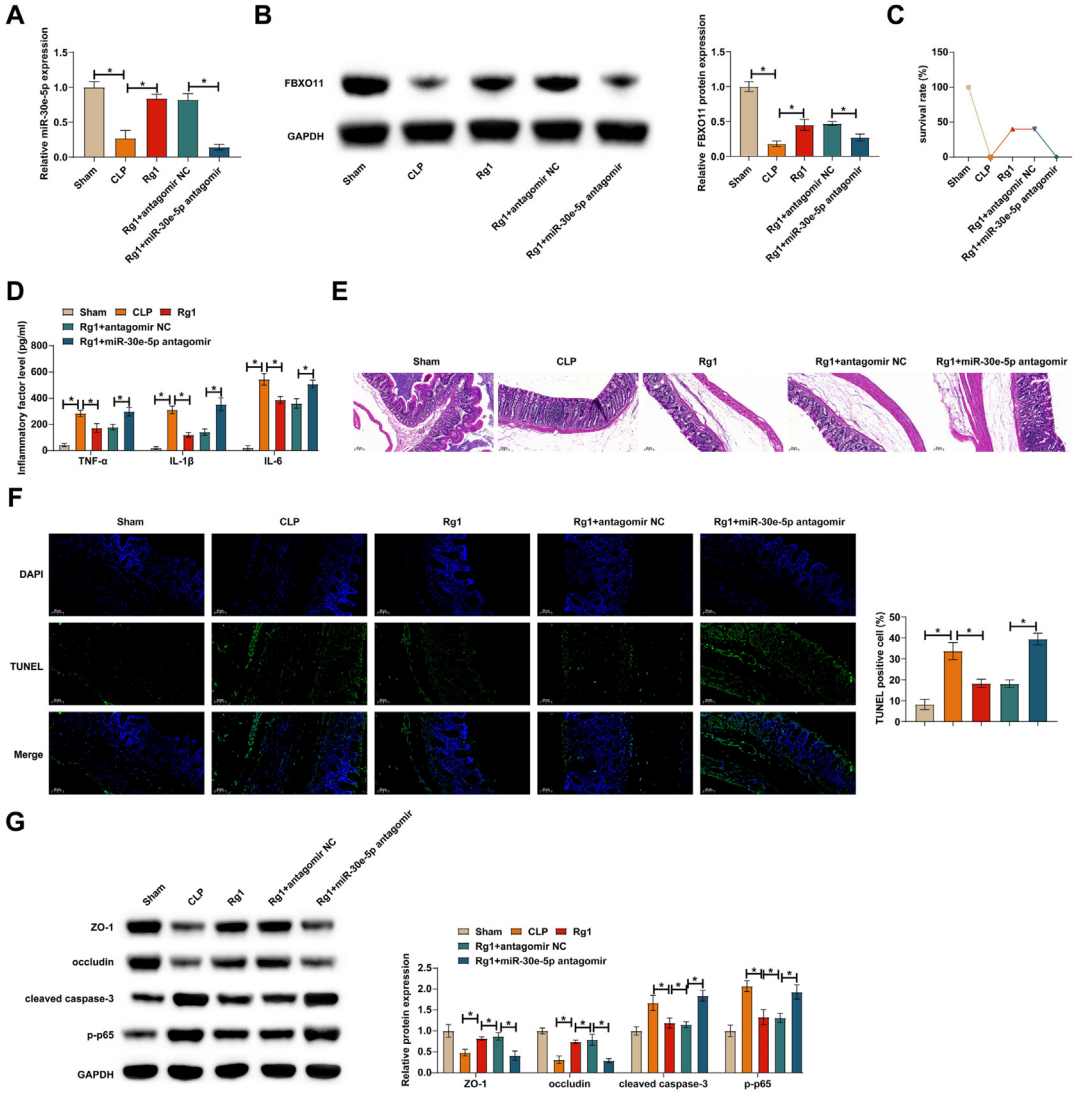

Fig. 6. Rg1 improves ClP-mediated impairment of intestinal barrier function by regulating miR-30e-5p/FBXO11 axis. Sepsis injury model was established by CLP, and Rg1 administration and miR-30e-5p antagomir injection were performed. (A) miR-30e-5p expression in colon tissues detected by RT-qPCR. (B) FBXO11 in mouse colon tissue detected by Western blot; (C) Analysis of mouse survival rate; (D) Serum LPS and colon tissue levels of inflammatory cytokines analyzed by commercial kits; (E) Representative images of colon tissue in mice stained by HE; (F) Representative TUNEL staining images of mouse colon tissue; (G) ZO-1, occludin, cleaved caspase-3, and p-p65 in mouse colon tissue detected by western blot. Data were expressed as mean ± SD (n = 10). * $P < 0.05$.

tic effect of Rg1 (Fig. 6E-F). Western blot manifested that Rg1 administration promoted ZO-1 and occludin expression, and inhibited cleaved caspase-3 and p-p65 expression, but these effects were rescued by downregulating miR-30e-5p (Fig. 6G).

4. Discussion

Sepsis-mediated systemic inflammation and multiple organ failure are the main causes of the high mortality rate [11]. Although many studies have reported that Rg1 has a healing effect on systemic injury caused by sepsis, the potential mechanism of Rg1 to improve sepia-mediated damage to intestinal barrier function needs to be further explored. Therefore, this study analyzed the mechanism by which Rg1 ameliorates septic intestinal barrier damage and confirmed that Rg1 administration can upregulate tmiR-30e-5p and downregulate FBXO11, thereby improving septic inflammation, apoptosis, and tight junction breakdown of intestinal epithelial cells.

Ginsenosides, its metabolites Rg1, compounds K, Rb1, Re, Rg3 and Rg5 regulate inflammation-related signals and reduce the level of pro-inflammatory cytokines to exert anti-inflammatory roles by binding to glucocorticoid receptors [12]. Rg1 as a beneficial plant extract has been found to be effective in improving sepsis-related injuries. inflammation. For example, Rg1 regulates SIRT1 by inhibiting endoplasmic reticulum stress and inflammation to improve septic inflammation and injury [10]. In addition, Rg1 inhibits septic myocardial inflammation [7] and alleviates sepsis-induced acute kidney injury by reducing ferroptosis of renal tubular epithelial cells [6]. Moreover, Rg1 has been determined to show alleviating effects on sepsis-induced cardiac dysfunction and mitochondrial dysfunction by activating the Akt/GSK-3β pathway [13]. Notably, it is reported that Rg1 can decrease the expression of inflammatory factors and reduce the apoptosis of hippocampal neurons, thus relieving sepsis-associated encephalopathy [14]. The current work found that Rg1 also inhibited septic intestinal inflammation, reduced levels of intestinal inflammatory factors and serum LPS, and inhibited the activation of the NF-κB pathway. After the treatment of CLP, the intestinal tight junctions are destroyed, and LPS infiltration through the portal vein in large quantities causes systemic inflammatory damage [13,15]. The current work found that Rg1 can protect intestinal epithelial tight junctions and promote the expression of tight junction proteins ZO-1 and occludin. This is of great benefit in preventing LPS from entering the bloodstream. The decrease of intestinal permeability and LPS content in systemic circulation may be important reasons for the treatment of systemic inflammation by Rg1.

This work analyzed downstream signaling pathways regulated by Rg1. miRNAs are involved in septic intestinal damage. For example, down-regulation of miR-155 blocks activation of the NF-κB signaling pathway, thereby alleviating septic inflammation and intestinal barrier dysfunction [16]. This study focused on a miRNA called miR-30e-5p. miR-30e-5p is abnormally low expressed in inflammations including myocardial infarction-mediated inflammation [9], cerebral ischemia mediated-neuroinflammation [17], and systemic lupus erythematosus mediated inflammation [18]. Functionally, overexpressing miR-30e-5p has the ability to reduce IL-1β, TNF-α, and IL-6 to suppress inflammation in H9c2 cells under hypoxia [19]. In rats after intracerebral hemorrhage, overexpression of miR-30e-5p inhibits neuronal inflammation while saving neuronal function [17]. This study found low expression of miR-30e-5p in intestinal cells and tissues after LPS and CLP treatment. Overexpressing miR-30e-5p improved LPS-mediated intestinal cell inflammation and intestinal tight junctions. In addition, the downstream target genes of miR-30e-5p were analyzed. Mechanistically, miR-30e-5p is reduced in expression after stimulation by inflammatory signals, which leads to increased expression of FBXO11. In chronic obstructive pulmonary disease, FBXO11 overexpression has been found to induce inflammatory response [20]. FXBO11 is a regulator of TGFβ pathway [21], which is considered significant for the proliferation and differentiation of immunoreactive cells [22]. Here, upregulating FBXO11 led to the activation of the NF-κB pathway and the release of inflammatory cytokines, which may be related to the activation of immune T cells during sepsis.

5. Conclusions

This study demonstrated that Rg1 improves septic intestinal barrier function impairment by regulating the miR-30e-5p/FBXO11 axis. Our findings provide a new scientific basis for the efficient utilization of Rg1 for intestinal damage in sepsis.

Ethical approval

All animal experiments were complied with the ARRIVE guidelines and performed in accordance with the National Institutes of Health Guide for the Care and Use of Laboratory Animals. The experiments were approved by the Institutional Animal Care and Use Committee of Changshu Hospital Affiliated to Nanjing University of Chinese Medicine.

Financial support

Changshu Municipal Health and Health Commission Science and Technology Plan Project in 2021 (Project No. CSWS202121).

Conflict of interests

The authors have no conflicts of interest to declare.

Data availability

The datasets used and/or analyzed during the present study are available from the corresponding author on reasonable request.

Author contributions

- Study conception and design: W Zhu; D Fan.
- Data collection: Z Zhou; Y Wang; X Huang; F Lu.
- Analysis and interpretation of results: L Zhang; D Wu; Y Ren; X Gao.
- Draft manuscript preparation: W Zhu; D Fan.
- Revision of the results and approved the final version of the manuscript: X Gao.

References

[1] Faix JD. Biomarkers of sepsis. Crit Rev Clin Lab Sci 2013;50(1):23–36. https://doi.org/10.3109/10408363.2013.764490. PMid: 23480440.
[2] Haussner F, Chakraborty S, Halbgebauer R, et al. Challenge to the intestinal mucosa during sepsis. Front Immunol 2019;10:891. https://doi.org/10.3389/fimmu.2019.00891. PMid: 31114571.
[3] Esposito S, De Simone G, Boccia G, et al. Sepsis and septic shock: New definitions, new diagnostic and therapeutic approaches. J Glob Antimicrob Resist 2017;10:204–12. https://doi.org/10.1016/j.jgar.2017.06.013. PMid: 28743646.
[4] Mancuso C, Santangelo R. *Panax ginseng* and *Panax quinquefolius*: From pharmacology to toxicology. Food Chem Toxicol 2017;107(Pt A):362–72. https://doi.org/10.1016/j.fct.2017.07.019. PMid: 28698154.

[5] Zhou P, Xie W, Sun Y, et al. Ginsenoside Rb1 and mitochondria: A short review of the literature. Mol Cell Probes 2019;43:1–5. https://doi.org/10.1016/j.mcp.2018.12.001. PMid: 30529056.
[6] Guo J, Wang R, Min F. Ginsenoside Rg1 ameliorates sepsis-induced acute kidney injury by inhibiting ferroptosis in renal tubular epithelial cells. J Leukoc Biol 2022;112(5):1065–77. https://doi.org/10.1002/JLB.1A0422-211R. PMid: 35774015.
[7] Luo M, Yan D, Sun Q, et al. Ginsenoside Rg1 attenuates cardiomyocyte apoptosis and inflammation via the TLR4/NF-kB/NLRP3 pathway. J Cell Biochem 2020;121(4):2994–3004. https://doi.org/10.1002/jcb.29556. PMid: 31709615.
[8] Zhang Y, Sun K, Liu YY, et al. Ginsenoside Rb1 ameliorates lipopolysaccharide-induced albumin leakage from rat mesenteric venules by intervening in both trans- and paracellular pathway. Am J Physiol Gastrointest Liver Physiol 2014;306(4):G289–300. https://doi.org/10.1152/ajpgi.00168.2013. PMid: 24356882.
[9] Chen YL, Xie YJ, Liu ZM, et al. Omega-3 fatty acids impair miR-1-3p-dependent Notch3 down-regulation and alleviate sepsis-induced intestinal injury. Mol Med 2022;28:9. https://doi.org/10.1186/s10020-021-00425-w. PMid: 35090386.
[10] Wang QL, Yang L, Peng Y, et al. Ginsenoside Rg1 regulates SIRT1 to ameliorate sepsis-induced lung inflammation and injury via inhibiting endoplasmic reticulum stress and inflammation. Mediators Inflamm 2019;2019:6453296. https://doi.org/10.1155/2019/6453296. PMid: 30918470.
[11] Rowe TA, McKoy JM. Sepsis in older adults. Infectious DiseasesClin North Am 2017;31(4):731–42. https://doi.org/10.1016/j.idc.2017.07.010. PMid: 29079157.
[12] Yu T, Tang Y, Zhang F, et al. Roles of ginsenosides in sepsis. J Ginseng Res 2023;47(1):1–8. https://doi.org/10.1016/j.jgr.2022.05.004. PMid: 36644389.
[13] Liu Z, Yang D, Gao J, et al. Discovery and validation of miR-452 as an effective biomarker for acute kidney injury in sepsis. Theranostics 2020;10 (26):11963–75. https://doi.org/10.7150/thno.50093. PMid: 33204323.
[14] Li Y, Wang F, Luo Y. Ginsenoside Rg1 protects against sepsis-associated encephalopathy through beclin 1-independent autophagy in mice. J Surg Res 2017;207:181–9. https://doi.org/10.1016/j.jss.2016.08.080. PMid: 27979475.
[15] Shen Y, Zhang Y, Du J, et al. CXCR5 down-regulation alleviates cognitive dysfunction in a mouse model of sepsis-associated encephalopathy: Potential role of microglial autophagy and the p38MAPK/NF-κB/STAT3 signaling pathway. J Neuroinflammation 2021;18:246. https://doi.org/10.1186/s12974-021-02300-1. PMid: 34711216.
[16] Cao YY, Wang Z, Wang ZH, et al. Inhibition of miR-155 alleviates sepsis-induced inflammation and intestinal barrier dysfunction by inactivating NF-κB signaling. Int Immunopharmacol 2021;90:107218. https://doi.org/10.1016/j.intimp.2020.107218. PMid: 33296782.
[17] Song H, Xu N, Jin S. miR-30e-5p attenuates neuronal deficit and inflammation of rats with intracerebral hemorrhage by regulating TLR4. Exp Ther Med 2022;24(2):492. https://doi.org/10.3892/etm.2022.11419. PMid: 35837037.
[18] Cheng T, Ding S, Liu S, et al. Resolvin D1 improves the Treg/Th17 imbalance in systemic lupus erythematosus through miR-30e-5p. Front Immunol 2021;12:668760. https://doi.org/10.3389/fimmu.2021.668760. PMid: 34093566.
[19] Chen Y, Yin Y, Jiang H. miR-30e-5p alleviates inflammation and cardiac dysfunction after myocardial infarction through targeting PTEN. Inflammation 2021;44(2):769–79. https://doi.org/10.1007/s10753-020-01376-w. PMid: 33180227.
[20] Mei J, Zhang Y, Lu S, et al. Long non-coding RNA NNT-AS1 regulates proliferation, apoptosis, inflammation and airway remodeling of chronic obstructive pulmonary disease *via* targeting miR-582-5p/FBXO11 axis. Biomed Pharmacother 2020;129:110326. https://doi.org/10.1016/j.biopha.2020.110326. PMid: 32768929.
[21] Rye MS, Wiertsema SP, Scaman ES, et al. FBXO11, a regulator of the TGFβ pathway, is associated with severe otitis media in Western Australian children. Genes Immun 2011;12(5):352–9. https://doi.org/10.1038/gene.2011.2. PMid: 21293382.
[22] Travis MA, Sheppard D. TGF-β activation and function in immunity. Annu Rev Immunol 2014;32:51–82. https://doi.org/10.1146/annurev-immunol-032713-120257. PMid: 24313777.